

Scalar-mediated $t\bar{t}$ forward-backward asymmetry

Kfir Blum, Yonit Hochberg and Yosef Nir

*Department of Particle Physics and Astrophysics
Weizmann Institute of Science,
Rehovot 76100, Israel*

kfir.blum,yonit.hochberg,yosef.nir@weizmann.ac.il

Abstract

A large forward-backward asymmetry in $t\bar{t}$ production, for large invariant mass of the $t\bar{t}$ system, has been recently observed by the CDF collaboration. Among the scalar mediated mechanisms that can explain such a large asymmetry, only the t -channel exchange of a color-singlet weak-doublet scalar is consistent with both differential and integrated $t\bar{t}$ cross section measurements. Constraints from flavor changing processes dictate a very specific structure for the Yukawa couplings of such a new scalar. No sizable deviation in the differential or integrated $t\bar{t}$ production cross section is expected at the LHC.

1 Introduction

The CDF collaboration has recently observed a large forward-backward $t\bar{t}$ production asymmetry for large invariant mass of the $t\bar{t}$ system [1]:

$$A_h^{t\bar{t}} \equiv A^{t\bar{t}}(M_{t\bar{t}} \geq 450 \text{ GeV}) = +0.475 \pm 0.114, \quad (1)$$

to be compared with the Standard Model (SM) prediction [2, 3, 4], $(A_h^{t\bar{t}})_{SM} = +0.09 \pm 0.01$. Eq. (1) updates (and is consistent with) previous CDF and D0 measurements of the inclusive asymmetry [5, 6]. Such a large effect is suggestive of an interference effect between a tree level exchange of a new boson with an electroweak-scale mass and the SM gluon-mediated amplitude. The intermediate boson could be either a vector-boson or a scalar. In this work, we focus on the latter possibility [7, 8, 9, 10, 11, 12, 13, 14, 15, 16, 17, 18, 19]. (For earlier work on scalar mediated mechanisms that give a large inclusive forward-backward asymmetry, see Refs. [20, 21, 22, 23, 24, 25].)

Eight scalar representations can interfere with the SM in $t\bar{t}$ production at the Tevatron:

$$(\bar{6}, 1)_{-\frac{4}{3}}, (\bar{6}, 1)_{-\frac{1}{3}}, (\bar{6}, 3)_{-\frac{1}{3}}, (3, 1)_{-\frac{4}{3}}, (3, 1)_{-\frac{1}{3}}, (3, 3)_{-\frac{1}{3}}, (8, 2)_{-\frac{1}{2}}, (1, 2)_{-\frac{1}{2}}. \quad (2)$$

In Section 2 we argue that only the color-singlet weak doublet $(1, 2)_{-\frac{1}{2}}$ can enhance $A_h^{t\bar{t}}$ without being inconsistent with existing measurements of the total $t\bar{t}$ production cross section or invariant mass distribution.

Guided by the top-related collider measurements, we focus our attention on the weak doublet. Given that $\mathcal{O}(1)$ coupling is required to either $u\bar{t}$ or $d\bar{t}$, the weak doublet cannot be the ordinary Higgs doublet, nor can it be incorporated into a two Higgs doublet model with ‘‘natural flavor conservation’’. It is thus clear that the scalar sector of the theory has a special flavor structure. In this work, we emphasize the interplay between the features required to explain the top-related measurements and the flavor constraints.

The plan of the sections investigating the color-singlet weak-doublet scalar is as follows. In Section 3 we introduce our notation and formalism for the investigation of the extra weak doublet. In Section 4 we show how flavor-related observables allow for only a very specific flavor structure of the scalar doublet. The implications for electroweak precision measurements are studied in Section 5, and for additional top-related observables in Section 6. We summarize our results in Section 7.

2 Top-related constraints

When new physics is invoked to account for the large value of $A_h^{t\bar{t}}$, one has to make sure that such new physics does not violate the constraints from other top-related measurements. Specifically, we consider the following measurements:

- (i) The forward-backward $t\bar{t}$ production asymmetry for small invariant mass of the $t\bar{t}$ system [1]:

$$A_l^{t\bar{t}} \equiv A^{t\bar{t}}(M_{t\bar{t}} \leq 450 \text{ GeV}) = -0.116 \pm 0.153, \quad (3)$$

to be compared with the SM prediction [2], $A_l^{t\bar{t}} = +0.040 \pm 0.006$.

- (ii) The $t\bar{t}$ differential cross section [26]. We represent this constraint by considering a particular $M_{t\bar{t}}$ bin:

$$\sigma_h \equiv \sigma^{t\bar{t}}(700 \text{ GeV} < M_{t\bar{t}} < 800 \text{ GeV}) = 80 \pm 37 \text{ fb}, \quad (4)$$

to be compared with the SM prediction [2, 27], $\sigma_h = 80 \pm 8 \text{ fb}$.

- (iii) The $t\bar{t}$ total production cross section measured at CDF [28],

$$\sigma_i \equiv \sigma_{\text{tot}}^{t\bar{t}} = 7.50 \pm 0.48 \text{ pb}, \quad (5)$$

consistent with D0 measurements [29]. Some controversy exists regarding the theoretical SM prediction. Ref. [30] obtains $\sigma_i = 7.2 \pm 0.4$ pb, consistent with previous results [31], but in some disagreement with Ref. [27] which obtains $\sigma_i = 6.5 \pm 0.3$ pb. In what follows, we conservatively allow a ${}^{+30\%}_{-10\%}$ uncertainty on the $t\bar{t}$ total production cross section.

For each of the eight representations of Eq. (2), only few parameters are relevant to the calculation of the $t\bar{t}$ production cross section and forward-backward asymmetry. Typically, these parameters include the mass M , a coupling $|\lambda|^2$, and the width Γ . In some cases, there is more than one coupling of relevance, forming a slightly more involved parameter space. In practice, in all cases we find that varying the width between $\Gamma = (0.01 - 0.5)M$ does not affect the results significantly. The most essential features, such as the sign of the leading interference terms with the SM diagrams and the possibility of forward-peaking kinematical features, are dictated purely by the choice of representation. This situation enables us to compute the top-related observables for each of the representations, and check for consistency with collider data, in a model-independent way.

The details of our calculation for each representation are given in App. A. We work at LO, using the MSTW2008 LO PDF set [32] and adopting renormalization scale and factorization scale $\mu_R = \mu_F = \sqrt{\tilde{s}}$, where \tilde{s} is the partonic center of mass energy. Where not stated otherwise, we use $\alpha_S(m_Z) = 0.139$. We estimate the uncertainties in our calculation by varying the renormalization and factorization scales within the range $(0.5\sqrt{\tilde{s}} - 2\sqrt{\tilde{s}})$, by comparing the results to results obtained using the CTEQ5M PDF set [33], and by varying the value of $\alpha_S(m_Z)$ in the range $(0.117 - 0.139)$. The largest uncertainties we find arise from varying α_S , leading to an uncertainty on $A^{t\bar{t}}$ which can be as large 10% – 30%, but is typically smaller. We checked that these uncertainties do not affect our conclusions. In order to minimize the impact of NLO corrections to the new physics (NP) contributions, we normalize the new physics contribution to the SM one [34]. We assume that the K -factors are universal, so that the NP/SM ratios at LO and NLO are the same.

We (conservatively) consider a parameter region as ruled out if any of the following conditions applies:

$$\begin{aligned}
A_{h,\text{NP}}^{t\bar{t}} &< 0.2, \\
A_{i,\text{NP}}^{t\bar{t}} &> 0.2, \\
N_h \equiv |\sigma_h^{\text{NP}}|/\sigma_h^{\text{SM}} &> 1, \\
N_i \equiv \sigma_i^{\text{NP}}/\sigma_i^{\text{SM}} &> +0.3 \text{ or } < -0.1.
\end{aligned} \tag{6}$$

Our main result is that, except from the color-singlet weak-doublet $(1,2)_{-1/2}$, all of the other scalar representations are ruled out from explaining the large forward-backward asymmetry Eq. (1). The reason is that all of the colored representations enhance the $t\bar{t}$ production cross section at low and/or high invariant mass, in conflict with experimental data. Thus, if the parameters relevant for these representations are tuned to pass the first criterion in Eq. (6), they inevitably fail on at least one of the last two criteria.

For the color sextet and triplet, this tension was mentioned in Refs. [7] and [9], respectively, but was not taken to imply that the models are excluded. It was also pointed out in Ref. [11].

In Table 1 we present, for each representation, the largest value of $A_{h,\text{NP}}^{t\bar{t}}$ which passes each of the remaining criteria of Eq. (6). A failure on any of these criteria is manifest through a value of $A_{h,\text{NP}}^{t\bar{t}} < 0.2$. A failure of a certain representation to account for the forward-backward asymmetry is manifest through at least one entry in the three columns that has $A_{h,\text{NP}}^{t\bar{t}} < 0.2$.

The small $(1,2)_{-1/2}$ parameter region which survives all of the conditions of Eq. (6) is shown in the left panel of Fig. 1. Here, the scalar couples the top to up quarks (see Section 3 for details on the scalar couplings). The allowed region, where large $A_h^{t\bar{t}}$ can be obtained without violating cross section constraints, has $M < 130$ GeV and $\mathcal{O}(1)$ coupling. (The fact that a color-singlet weak-doublet scalar can explain the CDF value of $A_h^{t\bar{t}}$ was first pointed out in Ref. [10]. They use methods of effective field theory, and thus do not derive bounds on the mass and couplings of the scalar.) Our results are consistent with the results of Refs. [14, 16, 17]. The allowed parameter region extends to low scalar mass, without conflict

Table 1: The maximum value of $A_{h,\text{NP}}^{t\bar{t}}$ for a given top-related constraint.

Irrep	$\max\{A_{h,\text{NP}}^{t\bar{t}} \mid N_h < 1\}$	$\max\{A_{h,\text{NP}}^{t\bar{t}} \mid -0.1 < N_i < +0.3\}$	$\max\{A_{h,\text{NP}}^{t\bar{t}} \mid A_{l,\text{NP}}^{t\bar{t}} < 0.2\}$
$(1, 2)_{-\frac{1}{2}} \text{ (u)}$	0.27	0.25	0.29
$(1, 2)_{-\frac{1}{2}} \text{ (d)}$	0.17	0.09	0.24
$(8, 2)_{-\frac{1}{2}} \text{ (u)}$	0.08	0.02	0.23
$(8, 2)_{-\frac{1}{2}} \text{ (d)}$	0.12	0.03	0.23
$(\bar{6}, 1)_{-\frac{1}{3}}$	0.17	0.19	0.44
$(\bar{6}, 3)_{-\frac{1}{3}}$	0.14	0.18	0.49
$(\bar{6}, 1)_{-\frac{4}{3}}$	0.14	0.18	0.50
$(3, 1)_{-\frac{1}{3}}$	0.17	0.27	0.44
$(3, 3)_{-\frac{1}{3}}$	0.11	0.42	0.55
$(3, 1)_{-\frac{4}{3}}$	0.10	0.41	0.55

with $t\bar{t}$ cross section measurements, due to interference with the SM s -channel gluon exchange diagram. The interference reduces the forward-backward symmetric and enhances the asymmetric production cross section. Considering LEP II searches we limit the discussion to scalar mass larger than 100 GeV. For M below m_t , top decay to the weak-doublet can effect the parameter space depicted in Fig. 1; See discussion in Section 6.2.

In the right panel of Fig. 1 we plot $A_h^{t\bar{t}}$ together with contours corresponding roughly to the 1σ allowed ranges for the cross sections and low bin asymmetry. We see that the low bin asymmetry places the tightest constraint on the doublet model. No parameter region is found with $A_h^{t\bar{t}} > 0.2$ and $A_l^{t\bar{t}} < 0.1$.

At the Tevatron, if the coupling involves right-handed up quarks (u-type), then $t\bar{t}$ production could feed off the $u\bar{u}$ and/or the $d\bar{d}$ luminosity. On the other hand, if the coupling involves right-handed down quarks (d-type), then $t\bar{t}$ production must feed off the $d\bar{d}$ luminosity. Since the $d\bar{d}$ luminosity makes up only $\lesssim 15\%$ of the $u\bar{u}$ luminosity at high invariant mass, producing $A_h^{t\bar{t}}$ via the d-type coupling requires a larger coupling for a given value of the scalar mass. Thus, the d-type coupling is more tightly constrained by the $t\bar{t}$ cross section measurements and, as can be seen in Table 1, it fails the N_i and N_h criteria of Eq. (6).

Despite this tension of d-type coupling with the $t\bar{t}$ cross section, in what follows we keep the d-type coupling in the discussion. We do this mainly to cover the possibility that both u- and d-type couplings occur in conjunction, leading to potential combined effects that could in principle broaden the allowed parameter range. Eventually, we will show that flavor constraints preclude this possibility.

It was pointed out in Refs. [11, 35] that models in which $t\bar{t}$ production proceeds via t -channel exchange can have sizable corrections to the parton level $t\bar{t}$ cross section, as deduced by CDF. While such acceptance issues are not relevant for the color sextet and triplet representations, the cross section constraints quoted here for the color singlet and octet could be somewhat over restrictive.¹ For the color singlet, these effects might extend the allowed parameter region depicted in Fig. 1 to include slightly larger values of M and λ . For the color octet, we have checked that even relaxing the total cross section constraint by a factor of three, would not allow to explain $A_h^{t\bar{t}}$ with $M > 100$ GeV.

Finally, we comment that the same interference mechanism which helps the color-singlet weak-doublet scalar evade the Tevatron constraints on the $t\bar{t}$ production cross section is at work also at the LHC. Thus, no sizable distortion of the differential or inclusive $t\bar{t}$ production cross section is expected at the LHC.

¹We thank Jure Zupan and Alex Kagan for discussions on this point.

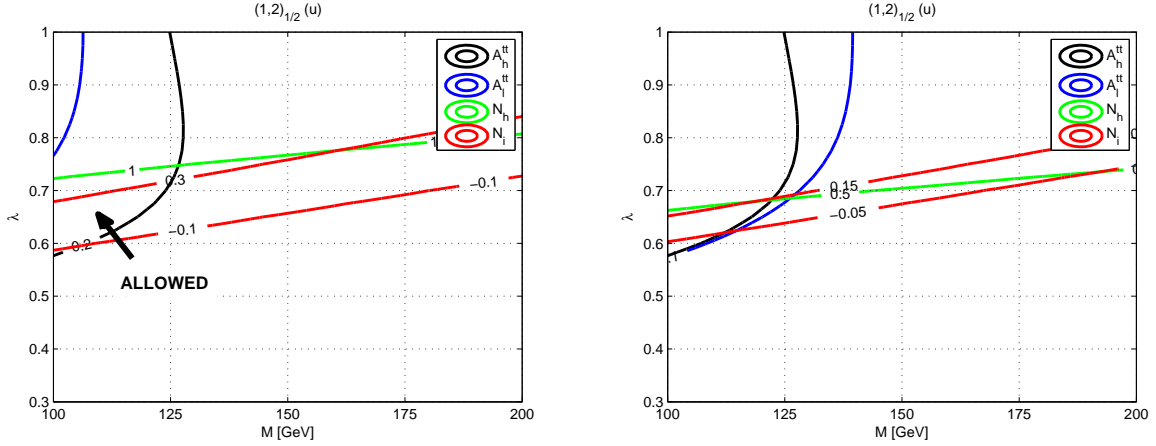


Figure 1: The $(M, |\lambda|)$ parameter space for the $(1, 2)_{-1/2}$ scalar, coupling the top to the up quark. Black (blue) curves correspond to $A_h^{t\bar{t}}$ ($A_l^{t\bar{t}}$). Green (red) curves correspond to N_h (N_i). Left panel: Parameter space allowed by Eq. (6). Here, the area below the black curve, the area above the blue curve, the area above the green curve and the area above the upper and inside the lower red curves are ruled out by $> 2\sigma$ by the corresponding observable. Right panel: Same as on the left, but limiting the deviations on $A_l^{t\bar{t}}$, N_h and N_i to $\lesssim 1\sigma$. No parameter region satisfies $A_h^{t\bar{t}} > 0.2$ and $A_l^{t\bar{t}} < 0.1$ while simultaneously satisfying cross section constraints at one sigma.

For instance, taking $\lambda = 0.7$ and $M = 120$ GeV, at the border of the allowed parameter space defined in Fig. 1, produces only a $\sim 30\%$ deviation in the differential $t\bar{t}$ cross section at $M_{t\bar{t}} = 1.5$ TeV at the LHC.

3 The weak doublet

We consider a weak doublet

$$\Phi \sim (1, 2)_{-1/2} = \begin{pmatrix} \phi^0 \\ \phi^- \end{pmatrix}. \quad (7)$$

This color-singlet can couple left-handed quarks to right-handed quarks in either the up or the down sector.

3.1 Coupling to right-handed up quarks

The relevant Lagrangian terms in the quark mass basis are given by

$$\mathcal{L}_u = -V(\Phi) + \left[2\phi^0 u_{Li}^\dagger X_{ij} u_{Rj} + 2\phi^- d_{Li}^\dagger (V^\dagger X)_{ij} u_{Rj} + \text{h.c.} \right], \quad (8)$$

where X is a complex 3×3 matrix in flavor space and $V = V_{\text{CKM}}$.

To account for the forward-backward asymmetry in $t\bar{t}$ production, Φ needs to have an $\mathcal{O}(1)$ coupling to $u\bar{t}$. There are two such possibilities: $X_{13} = \mathcal{O}(1)$ and/or $X_{31} = \mathcal{O}(1)$. Indeed, from Fig. 1 we learn that $A_h^{t\bar{t}} > 0.2$ implies

$$|\lambda| > 0.6, \quad M < 130 \text{ GeV}, \quad (9)$$

where λ refers to either X_{13} or X_{31} . We could expect that a smaller λ is allowed in case that both X_{13} and X_{31} exist with similar magnitude. We will see, however, that flavor constraints imply $|X_{13}| \ll 1$, and so in practice this case cannot occur.

Since a left-handed quark doublet is involved in the Lagrangian (8), there is often an interesting interplay between flavor constraints from the up and the down sector (see, for example, [36]). In what follows, in order to explore this interplay, we consider four different structures for X :

$$X = \lambda \begin{pmatrix} 0 & 0 & 0 \\ 0 & 0 & 0 \\ 1 & 0 & 0 \end{pmatrix}, \quad V^\dagger X = \lambda \begin{pmatrix} V_{td}^* & 0 & 0 \\ V_{ts}^* & 0 & 0 \\ V_{tb}^* & 0 & 0 \end{pmatrix} \quad \text{case I,} \quad (10)$$

$$X = \lambda \begin{pmatrix} V_{ub} & 0 & 0 \\ V_{cb} & 0 & 0 \\ V_{tb} & 0 & 0 \end{pmatrix}, \quad V^\dagger X = \lambda \begin{pmatrix} 0 & 0 & 0 \\ 0 & 0 & 0 \\ 1 & 0 & 0 \end{pmatrix} \quad \text{case II,} \quad (11)$$

$$X = \lambda \begin{pmatrix} 0 & 0 & 1 \\ 0 & 0 & 0 \\ 0 & 0 & 0 \end{pmatrix}, \quad V^\dagger X = \lambda \begin{pmatrix} 0 & 0 & V_{ud}^* \\ 0 & 0 & V_{us}^* \\ 0 & 0 & V_{ub}^* \end{pmatrix} \quad \text{case III,} \quad (12)$$

$$X = \lambda \begin{pmatrix} 0 & 0 & V_{ud} \\ 0 & 0 & V_{cd} \\ 0 & 0 & V_{td} \end{pmatrix}, \quad V^\dagger X = \lambda \begin{pmatrix} 0 & 0 & 1 \\ 0 & 0 & 0 \\ 0 & 0 & 0 \end{pmatrix} \quad \text{case IV.} \quad (13)$$

When there is a single entry in X , ϕ^0 couples to a single pair of up-type (mass eigenstate) quarks, but ϕ^- couples an up-type quark to all three down-type quarks. In contrast, when there is a single entry in $V^\dagger X$, ϕ^- couples to a single up-down pair, while ϕ^0 couples a single right-handed up-type quark to all three left-handed up-type quarks. Consequently, a single entry in X is subject to flavor constraints from the down sector, while a single entry in $V^\dagger X$ is subject to flavor constraints from the up sector.

In general, if both case I and case II are excluded, then so will be all intermediate cases, where both X_{31} and $(V^\dagger X)_{31}$ are $\mathcal{O}(1)$. Similarly, in general, if both case III and case IV are excluded, then so will be all intermediate cases, where both X_{13} and $(V^\dagger X)_{13}$ are $\mathcal{O}(1)$. Exceptions to these statements might arise in cases that there are cancellations between various contributions to flavor changing processes. Such cancellations indeed occur in MFV models [37].

3.2 Coupling to right-handed down quarks

The relevant Lagrangian terms in the quark mass basis are given by

$$\mathcal{L}_d = -V(\Phi) + \left[2\phi^+ u_{Li}^\dagger \tilde{X}_{ij} d_{Rj} - 2\phi^{0*} d_{Li}^\dagger (V^\dagger \tilde{X})_{ij} d_{Rj} + \text{h.c.} \right], \quad (14)$$

where \tilde{X} is a complex 3×3 matrix in flavor space and $V = V_{\text{CKM}}$.

Here there are only two different structures for \tilde{X} to consider:

$$\tilde{X} = \tilde{\lambda} \begin{pmatrix} 0 & 0 & 0 \\ 0 & 0 & 0 \\ 1 & 0 & 0 \end{pmatrix}, \quad V^\dagger \tilde{X} = \tilde{\lambda} \begin{pmatrix} V_{td}^* & 0 & 0 \\ V_{ts}^* & 0 & 0 \\ V_{tb}^* & 0 & 0 \end{pmatrix} \quad \text{case V,} \quad (15)$$

$$\tilde{X} = \tilde{\lambda} \begin{pmatrix} V_{ub} & 0 & 0 \\ V_{cb} & 0 & 0 \\ V_{tb} & 0 & 0 \end{pmatrix}, \quad V^\dagger \tilde{X} = \tilde{\lambda} \begin{pmatrix} 0 & 0 & 0 \\ 0 & 0 & 0 \\ 1 & 0 & 0 \end{pmatrix} \quad \text{case VI,} \quad (16)$$

analogous to Eqs. (10) (case I) and (11) (case II) above. Structures analogous to the cases III and IV in Eqs. (12) and (13) are irrelevant here as they do not couple the top quark to the light quarks.

To generate a sizable forward-backward asymmetry in $t\bar{t}$ production, the coupling between Φ and $d\bar{t}$ should be of order one, $\tilde{\lambda} = \mathcal{O}(1)$. As seen in Table 1, however, if the Lagrangian contains only the coupling in Eq. (14) then a large forward-backward asymmetry cannot be attained without violating cross section constraints.

4 Flavor constraints

In this section, we denote the masses of both the neutral and charged components of the scalar doublet by M . As will be seen in Section 5.1, the electroweak T -parameter constrains the splitting within the doublet such that the use of single scale M is valid for our discussion of flavor constraints.

4.1 Meson mixing

Scalar exchange can contribute to neutral meson mixing at tree level and via box diagrams. However, in all the cases that we consider, the constraints from tree level exchange are irrelevant. We thus focus on the loop contributions. These include box diagrams with two scalars and in some cases box diagrams with one scalar and one gauge or goldstone boson. In all of the cases relevant for our scenario, the mixed scalar-gauge diagrams, if exist, are parametrically suppressed by either a small quark mass insertion or by CKM factors compared to the diagrams with two internal scalars.

The strongest constraints on our scenarios arise from the K and D systems. Using the analysis of Ref. [38], we obtain the following constraints on (the absolute value of) our model parameters:

- $D^0 - \bar{D}^0$ mixing:

$$\frac{1}{32\pi^2} \left(\frac{M}{\text{TeV}} \right)^{-2} \sum_i \mathcal{F} \left(\frac{m_{u_i}^2}{M^2} \right) X_{1i}^2 X_{2i}^{*2} < 7 \times 10^{-7}. \quad (17)$$

- $K^0 - \bar{K}^0$ mixing:

$$\frac{1}{32\pi^2} \left(\frac{M}{\text{TeV}} \right)^{-2} \sum_i \mathcal{F} \left(\frac{m_{u_i}^2}{M^2} \right) (V^\dagger X)_{1i}^2 (V^\dagger X)_{2i}^{*2} < 10^{-6}. \quad (18)$$

The loop function \mathcal{F} is given by

$$\mathcal{F}(r) = \frac{1 - r^2 + 2r \ln r}{(1 - r)^3}. \quad (19)$$

The function \mathcal{F} obeys $\mathcal{F}(1) = \frac{1}{3}$, $\mathcal{F}(0) = 1$. Constraints on the couplings of Eq. (14) are obtained by replacing $m_{u_i} \rightarrow m_{d_i}$ and $X \rightarrow \tilde{X}$ in Eqs. (17) and (18). Somewhat stronger constraints apply from CP violation in the neutral D and K systems, if one assume phases of order one in the relevant scalar couplings.

The constraint (17) is relevant, in principle, to cases II, IV and (with the above mentioned modification) VI. The constraint (18) is relevant, in principle, to cases I, III and (with the above mentioned modification) V.

For cases I and V, the contribution to $K^0 - \bar{K}^0$ is suppressed by the small CKM combination $(V_{td}V_{ts}^*)^2$. Consequently, these cases remain unconstrained in the region of parameter space relevant for the forward-backward asymmetry. For cases II and VI, the contribution to $D^0 - \bar{D}^0$ is suppressed by the small CKM combination $(V_{ub}V_{cb}^*)^2$. Consequently, also these cases remain unconstrained in the region of parameter space relevant for the forward-backward asymmetry. These statements are valid even when taking into account the constraints from CP violation in the K and D systems.

For case III, the constraint from $K^0 - \bar{K}^0$ mixing reads

$$|\lambda|^4 \mathcal{F} \left(\frac{m_t^2}{M^2} \right) < 4 \times 10^{-4} \left(\frac{M}{250 \text{ GeV}} \right)^2, \quad (20)$$

thus ruling out case III from explaining the $A_h^{t\bar{t}}$. (To the best of our understanding, the model of Ref. [14] violates the constraint (20) by two orders of magnitude and is therefore excluded.)

For case IV, the constraint from $D^0 - \bar{D}^0$ mixing reads

$$|\lambda|^4 \mathcal{F} \left(\frac{m_t^2}{M^2} \right) < 2.7 \times 10^{-4} \left(\frac{M}{250 \text{ GeV}} \right)^2, \quad (21)$$

thus ruling out case IV from explaining the $A_h^{t\bar{t}}$.

4.2 Anomalous B decays

Anomalous b decays proceed via tree level exchange of the charged scalar, with

$$\mathcal{H}_{\text{eff}} \supset -\frac{4}{M^2} (X^\dagger V)_{ji}^* (X^\dagger V)_{k3} \left(d_{Li}^\dagger u_{Rj} \right) \left(u_{Rk}^\dagger b_L \right) + \text{h.c.}, \quad (22)$$

or via exchange of the neutral scalar, with

$$\mathcal{H}_{\text{eff}} \supset -\frac{4}{M^2} (\tilde{X}^\dagger V)_{ji}^* (\tilde{X}^\dagger V)_{k3} \left(d_{Li}^\dagger d_{Rj} \right) \left(d_{Rk}^\dagger b_L \right) + \text{h.c.}, \quad (23)$$

where brackets denote $\text{SU}(3)_c$ singlets. Of particular interest are the charmless decays, $b \rightarrow u\bar{u}d$, $b \rightarrow u\bar{u}s$, $b \rightarrow d\bar{d}d$ and $b \rightarrow d\bar{d}s$.

Among the four limiting cases remaining to consider [cases I (10), II (11), V (15) and VI (16)] only in cases I and V there is a ϕ -mediated tree level contribution to the decays considered here. In cases II and VI the scalar component coupling to the bottom quark ($\phi^- \bar{b}_L u_R$ or $\phi^{0*} \bar{b}_L d_R$) has no additional coupling to quarks, and consequently these cases are unconstrained by B decays.

We calculate the scalar-mediated contributions to B -meson decays into the seven final states, $\pi^+ \pi^-$, $\pi^- \pi^0$, $\pi^0 \pi^0$, $\pi^- \bar{K}^0$, $\pi^0 K^-$, $\pi^+ K^-$ and $\pi^0 \bar{K}^0$. We use the operator basis as defined in Ref. [39]. At the scale M , the effective Hamiltonian terms (22) and (23) correspond to the $\mathcal{O}_6^{(i)}$ and $\mathcal{O}_8^{(i)}$ operators,

$$\mathcal{O}_6^{(i)} = 4 \sum_{q=u,d} (\bar{b}_L^\alpha \gamma^\mu d_{Li\beta}) \left(\bar{q}_R^\beta \gamma_\mu q_{R\alpha} \right), \quad \mathcal{O}_8^{(i)} = 4 \sum_{q=u,d} \frac{3e_q}{2} (\bar{b}_L^\alpha \gamma^\mu d_{Li\beta}) \left(\bar{q}_R^\beta \gamma_\mu q_{R\alpha} \right), \quad (24)$$

where $\mathcal{H}_{\text{eff}} \supset \sum_i (z_6^{(i)} \mathcal{O}_6^{(i)} + z_8^{(i)} \mathcal{O}_8^{(i)})$. In case I, these operators are generated with coefficients

$$\delta z_6^{(i)}(M) \approx \frac{G_F}{3\sqrt{2}} \left(\frac{M}{250 \text{ GeV}} \right)^{-2} (X^\dagger V)_{1i} (X^\dagger V)_{13}^*, \quad (25a)$$

$$\delta z_8^{(i)}(M) \approx \frac{2G_F}{3\sqrt{2}} \left(\frac{M}{250 \text{ GeV}} \right)^{-2} (X^\dagger V)_{1i} (X^\dagger V)_{13}^*. \quad (25b)$$

In case V, these operators are generated with coefficients

$$\delta z_6^{(i)}(M) \approx \frac{2G_F}{3\sqrt{2}} \left(\frac{M}{250 \text{ GeV}} \right)^{-2} (\tilde{X}^\dagger V)_{1i} (\tilde{X}^\dagger V)_{13}^*, \quad (26a)$$

$$\delta z_8^{(i)}(M) \approx -\frac{2G_F}{3\sqrt{2}} \left(\frac{M}{250 \text{ GeV}} \right)^{-2} (\tilde{X}^\dagger V)_{1i} (\tilde{X}^\dagger V)_{13}^*. \quad (26b)$$

Table 2: Branching ratios for the relevant charmless B decays. For the experimental result, we provide the central value [42]. The experimental errors are at most of order 10%. For case I, the results scale with $|\lambda|^4 \left(\frac{M}{250 \text{ GeV}}\right)^{-4}$, where M is the mass of the charged scalar. For case V, the results scale with $|\tilde{\lambda}|^4 \left(\frac{M}{250 \text{ GeV}}\right)^{-4}$, where M is the mass of the neutral scalar.

Branching ratio	Exp. value	case I	case V
$\overline{B}^0 \rightarrow \pi^+ \pi^-$	5.1×10^{-6}	2.0×10^{-4}	6.9×10^{-7}
$B^- \rightarrow \pi^- \pi^0$	5.7×10^{-6}	5.9×10^{-5}	5.9×10^{-5}
$\overline{B}^0 \rightarrow \pi^0 \pi^0$	1.6×10^{-6}	6.5×10^{-6}	4.8×10^{-5}
$B^- \rightarrow \pi^- \overline{K}^0$	2.3×10^{-5}	7.4×10^{-6}	4.7×10^{-3}
$B^- \rightarrow \pi^0 K^-$	1.3×10^{-5}	1.2×10^{-3}	1.5×10^{-4}
$\overline{B}^0 \rightarrow \pi^+ K^-$	1.9×10^{-5}	4.6×10^{-3}	1.6×10^{-5}
$\overline{B}^0 \rightarrow \pi^0 \overline{K}^0$	9.5×10^{-6}	1.7×10^{-4}	1.0×10^{-3}

QCD running from the scale M down to the scale m_B is captured at leading log approximation (LLA) [40] by ($i = d, s$)

$$\delta z_6^{(i)}(m_B) \approx 1.5 \delta z_6^{(i)}(M), \quad \delta z_8^{(i)}(m_B) \approx 1.7 \delta z_8^{(i)}(M). \quad (27)$$

In addition, operator mixing at the ten percent level is induced, and is taken into account in our numerical calculations. We compute the relevant branching ratios using QCD factorization [41].

Comparing the flavor factor in the ϕ -mediated diagrams to that in the W -mediated tree level diagrams, we observe that the former is mildly enhanced in $b \rightarrow u\bar{u}d$, but strongly enhanced in $b \rightarrow u\bar{u}s$:

$$\left| \frac{V_{tb}V_{td}}{V_{ub}V_{ud}} \right| \sim 2.5, \quad \left| \frac{V_{tb}V_{ts}}{V_{ub}V_{us}} \right| \sim 50. \quad (28)$$

In Table 2 we provide a full list of the branching ratios for the relevant B decays. For each process, we present the experimental value, taken from Ref. [42], and the scalar-mediated contributions calculated for $M = 250 \text{ GeV}$ and $|\lambda| = 1$.

In case I, in all modes except $B^- \rightarrow \overline{K}^0 \pi^-$, the ϕ -mediated contribution, with $|\lambda|^2 \left(\frac{M}{250 \text{ GeV}}\right)^{-2} = \mathcal{O}(1)$, as required to explain $A_h^{t\bar{t}}$, is significantly larger than the experimental value. The strongest enhancement applies to $\text{BR}(\overline{B}^0 \rightarrow \pi^+ K^-)$, where the scalar contribution is a factor of about 240 above experimental bounds. The flavor ratio in Eq. (28) provides an enhancement of about three orders of magnitude, but the heavier scalar mass sets off part of this enhancement. (To the best of our understanding, the model of Ref. [14] enhances the $b \rightarrow u\bar{u}s$ transitions by about two orders of magnitude and is therefore excluded. This point was made in Ref. [15] which considers, however, the branching ratio for $B^+ \rightarrow \pi^+ K^0$. This decay is a $b \rightarrow d\bar{d}s$ transition that is only generated by RGE effects. Thus this channel puts only mild constraints on the model, in comparison to $b \rightarrow u\bar{u}s$ transitions.)

In case V, in all modes except $\overline{B}^0 \rightarrow \pi^+ \pi^-$ and $\overline{B}^0 \rightarrow \pi^+ K^-$, the scalar-mediated contribution, with $|\tilde{\lambda}|^2 \left(\frac{M}{250 \text{ GeV}}\right)^{-2} = \mathcal{O}(1)$, as required to explain $A_h^{t\bar{t}}$, is significantly larger than the experimental value. The strongest enhancement applies to $\text{BR}(B^- \rightarrow \overline{K}^0 \pi^-)$, where the scalar contribution is enhanced by a factor of about 200 above the experimental bound.

We conclude that charmless B decays exclude the possibility that $A_h^{t\bar{t}}$ is accounted for by a weak doublet scalar with couplings of type I or V. We thus find that only cases II and VI survive the constraints from flavor changing processes and can provide a viable mechanism for $A_h^{t\bar{t}}$.

In principle, we can consider the scalar couplings of cases II and VI simultaneously. The relevant part of the Lagrangian is then:

$$\begin{aligned}\mathcal{L} &\supset 2\lambda q_{L3}^\dagger \Phi u_R + \tilde{\lambda} q_{L3}^\dagger \tilde{\Phi} d_R + \text{h.c.} \\ &= 2\lambda(u_{L_i}^\dagger V_{ib} \phi^0 u_R + b_L^\dagger \phi^- u_R) + 2\tilde{\lambda}(u_{L_i}^\dagger V_{ib} \phi^+ d_R - b_L^\dagger \phi^{0*} d_R) + \text{h.c.}\end{aligned}\quad (29)$$

Integrating out the scalar field, we get (among others) the following interesting four-quark terms:

$$\mathcal{L}_{\text{eff}} = \frac{\lambda \tilde{\lambda} V_{ib}}{m_+^2} (b_L^\dagger u_R)(u_{L_i}^\dagger d_R) - \frac{\lambda \tilde{\lambda} V_{ib}}{m_0^2} (b_L^\dagger d_R)(u_{L_i}^\dagger u_R), \quad (30)$$

where m_0 and m_+ denote the masses of, respectively, the neutral and charged scalars. These terms lead, in particular, to $b \rightarrow u\bar{c}d$ decays, with CKM suppression by a factor of $V_{cb} \sim 0.04$. In contrast, within the SM, the W -mediated diagram is CKM suppressed by $V_{ub}V_{cd} \sim 0.0008$, a factor of 50 smaller.

The hadronic modes that are described by this ‘‘wrong sign’’ quark transition are $B^+ \rightarrow D^+\pi^0$, $B^+ \rightarrow D^0\pi^+$, $B^0 \rightarrow D^0\pi^0$, $B^0 \rightarrow D^+\pi^-$ and the analogous modes with $D \rightarrow D^*$ and/or with $\pi \rightarrow \rho$. (Of course, charge-conjugate modes are implied.)

In the PDG [42], one finds only a single attempt to measure one of these modes² [44]

$$\text{BR}(B^+ \rightarrow D^{*+}\pi^0) < 3.6 \times 10^{-6}. \quad (31)$$

The SM expectation, based on extracting the parameter r ,

$$r \equiv \sqrt{\frac{\tau_0}{\tau_+} \frac{2 \text{BR}(B^+ \rightarrow D^{*+}\pi^0)}{\text{BR}(B^0 \rightarrow D^{*-}\pi^+)}} , \quad (32)$$

from isospin relation and two measured branching fractions,

$$r = \tan \theta_c \frac{f_{D^*}}{f_{D_s^*}} \sqrt{\frac{\text{BR}(B^0 \rightarrow D_s^{*+}\pi^-)}{\text{BR}(B^0 \rightarrow D^{*-}\pi^+)}} \approx 0.02, \quad (33)$$

and on $\tau_+/\tau_0 = 1.071 \pm 0.009$ and $\text{BR}(B^0 \rightarrow D^{*-}\pi^+) = (2.76 \pm 0.21) \times 10^{-3}$, is

$$\text{BR}(B^+ \rightarrow D^{*+}\pi^0)^{\text{SM}} \approx 5.9 \times 10^{-7}. \quad (34)$$

Additional support that the $b \rightarrow u\bar{c}d$ transitions are doubly Cabibbo suppressed (DCS) can be found in [45], reporting on measuring CP violation in the Cabibbo favored (CF) modes $B^0 \rightarrow D^{*-}\pi^+$ and $B^0 \rightarrow D^-\pi^+$. In their Fig. 11, one can read an upper bound of order a few percent on the ratio between the DCS and CF amplitudes for each of the two cases.

Comparing the experimental bound (31) to the SM prediction (34), we conclude that the rate is enhanced by no more than a factor of order 6, while Eq. (30) predicts enhancement by about two-to-three orders of magnitude,

$$\begin{aligned}\frac{\Gamma(B^+ \rightarrow D^{*+}\pi^0)^\Phi}{\Gamma(B^+ \rightarrow D^{*+}\pi^0)^{\text{SM}}} &\approx \frac{|\lambda \tilde{\lambda}|^2}{g^4} \left| \frac{V_{cb}}{V_{ub}V_{cd}} \right|^2 \left(\frac{m_W}{m_0} \right)^4 \left(\frac{\langle D^{*+}\pi^0 | (b_L^\dagger d_R)(c_L^\dagger u_R) | B^0 \rangle}{\langle D^{*+}\pi^0 | (b_L^\dagger \gamma_\mu u_L)(c_L^\dagger \gamma^\mu d_L) | B^0 \rangle} \right)^2 \\ &\sim 2500 \frac{|\lambda \tilde{\lambda}|^2}{g^4} \left(\frac{m_W}{m_0} \right)^4.\end{aligned}\quad (35)$$

²Note that the range quoted, $\text{BR}(B^0 \rightarrow D^+\pi^-) = (4.6 \pm 0.4) \times 10^{-5}$, is *not* an experimental measurement, but rather a theoretical calculation based on a measurement of the $D_s^+\pi^-$ mode [43].

Thus, simultaneous order one couplings to both the up-quark (case II) and down-quark (case VI) are excluded.

In Section 2 we concluded that, in order to account for $A_h^{t\bar{t}}$, the scalar doublet should have order one couplings to the top and a first generation quark. In this section we found that coupling to the first generation quark doublet should be avoided. The order one coupling can be to either u_R or d_R , but not to both. In the language of our six limiting cases, only one of the two types II or VI is allowed by flavor constraints.

5 Electroweak constraints

5.1 The S and T parameters

The weak doublet can contribute to the electroweak S and T parameters. The PDG constraints read [42]

$$S = 0.01 \pm 0.10(-0.08), \quad (36)$$

$$T = 0.03 \pm 0.11(+0.09). \quad (37)$$

The central values corresponds to $m_h = 117$ GeV, while the shifts in parenthesis corresponds to $m_h = 300$ GeV.

We use the expressions for T and S in two Higgs doublet models from Ref. [46]. Taking the approximation of non-mixed neutral scalars, where one is degenerate with m_h and the others have a common mass m_0 , and denoting the mass of the charged component by m_+ , we have

$$T = \frac{1}{8\pi s_W^2 m_W^2} \left(\frac{m_0^2 + m_+^2}{2} - \frac{m_0^2 m_+^2}{m_+^2 - m_0^2} \ln \frac{m_+^2}{m_0^2} \right), \quad (38)$$

$$S = \frac{1}{24\pi} [(s_W^2 - c_W^2)^2 G(z_+, z_+) + G(z_0, z_0)], \quad (39)$$

where

$$z_a \equiv m_a^2/m_Z^2, \quad (40)$$

$$G(x, y) = -\frac{16}{3} + 5(x+y) - 2(x-y)^2 + 3 \left[\frac{x^2 + y^2}{x-y} - x^2 + y^2 + \frac{(x-y)^3}{3} \right] \ln \frac{x}{y} \\ + [1 - 2(x+y) + (x-y)^2] f(x+y-1, 1 - 2(x+y) + (x-y)^2), \quad (41)$$

$$f(z, w) = \begin{cases} \sqrt{w} \ln \left| \frac{z - \sqrt{w}}{z + \sqrt{w}} \right| & w > 0, \\ 0 & w = 0, \\ 2\sqrt{-w} \arctan \frac{\sqrt{-w}}{z} & w < 0. \end{cases}$$

The S parameter provides no meaningful constraint on the parameters of our model. The T parameter, on the other hand, constrains the mass splitting within the scalar doublet. The 2σ range for T gives a conservative bound on the maximal allowed mass splitting:

$$\left| \frac{m_+ - m_0}{M} \right| \lesssim 0.45 \frac{250 \text{ GeV}}{M}, \quad (42)$$

where $M = \frac{1}{2}(m_+ + m_0)$. For case II (VI), $A_h^{t\bar{t}}$ restricts the mass m_0 (m_+). Then, the T constraint of Eq. (42) allows the mass m_+ (m_0) to be shifted from m_0 (m_+) by at most ~ 110 GeV. These results are consistent with [47].

Explaining $A_h^{t\bar{t}}$ requires the mass of the relevant weak-doublet component to be in the range 100 – 130 GeV. Thus, we can now justify neglecting the mass splitting between the weak-doublet components in the discussion of flavor constraints in Section 4 and the use of the benchmark value of 250 GeV:

- In cases III and IV, $A^{t\bar{t}}$ is generated by the exchange of both the neutral and the charged scalars, and so neglecting the mass splitting in the meson-mixing analysis, which led to their exclusion, is justified.
- In cases I and V, $A^{t\bar{t}}$ is generated by the exchange of one component while meson-mixing and B decays are sensitive to the mass of the other scalar component. There, the T -parameter serves to restrict the splitting so that the analysis is valid.
- In cases II and VI, meson-mixing is generated by the same scalar component responsible for $A^{t\bar{t}}$ and there is no ambiguity. In the case where couplings of both type II and VI exist, the mixed B decays are sensitive to the masses of both scalar components. The use of a single benchmark mass value in the analysis is valid and the net result is unaltered.

5.2 R_b

Contributions to $Z \rightarrow b_L \bar{b}_L$ can arise from $(V^\dagger X)_{3i}$ or $(V^\dagger \tilde{X})_{3i}$ ($i = 1, 2, 3$) couplings via one loop diagrams with an internal quark and scalar. In cases II and VI, only the $i = 1$ terms exist. Explicitly, for case II the relevant coupling is $\lambda = (V^\dagger X)_{31}$ and the internal quark is u_R , while in case VI the relevant coupling is $\tilde{\lambda} = (V^\dagger \tilde{X})_{31}$ and the internal quark is d_R .

We denote the intermediate quark masses by m_u and m_d and the tree level Z couplings to the different particles by g_{d_L} , g_{u_R} , g_{d_R} , g_{ϕ^-} and g_{ϕ^0} . We neglect terms of $\mathcal{O}(m_b/M)$ and use $g_{u_R} + g_{\phi^-} - g_{d_L} = 0$ and $g_{d_R} - g_{\phi^0} - g_{d_L} = 0$.

To leading order in $|\lambda|^2/(4\pi)^2$, we obtain the effective shift to the $Z_\mu \bar{b}_L \gamma^\mu b_L$ vertex for case II:

$$\begin{aligned} \left. \frac{\delta g_{d_L}}{g_{d_L}} \right|_{\text{II}} &= \frac{4|\lambda|^2}{(4\pi)^2} \mathcal{F}'(r_Z, r_u), \\ \mathcal{F}'(r_Z, r_u) &= \int dx x \ln \left(\frac{\Delta_c}{M^2} \right) \\ &\quad - \int dx dy dz \delta(x+y+z-1) \left[\frac{g_{u_R}}{g_{d_L}} \left(\ln \left(\left| \frac{\Delta_a}{M^2} \right| \right) + \frac{zyr_Z}{\Delta_a} + 1 \right) + \frac{g_{\phi^-}}{g_{d_L}} \ln \left(\left| \frac{\Delta_b}{M^2} \right| \right) \right]. \end{aligned} \quad (43)$$

with

$$\begin{aligned} \frac{\Delta_c}{M^2} &= x + r_u(1-x), \quad \frac{\Delta_a}{M^2} = \frac{\Delta_c}{M^2} - r_Z zy, \quad \Delta_b = \Delta_a(x \leftrightarrow 1-x), \\ r_u &= m_u^2/M^2, \quad r_Z = m_Z^2/M^2. \end{aligned} \quad (44)$$

For case VI, we obtain

$$\left. \frac{\delta g_{d_L}}{g_{d_L}} \right|_{\text{VI}} = \left. \frac{\delta g_{d_L}}{g_{d_L}} \right|_{\text{II}} (\lambda \rightarrow \tilde{\lambda}, m_u \rightarrow m_d, g_{u_R} \rightarrow g_{d_R}, g_{\phi^-} \rightarrow -g_{\phi^0}). \quad (45)$$

In addition to the shift Eq. (43) (or (45)), the new scalars introduce tensor as well as imaginary vector terms to the $Z \rightarrow b_L \bar{b}_L$ amplitude. Since these other terms do not interfere with the leading SM diagram, they contribute only at next order in $\frac{|\lambda|^2}{(4\pi)^2}$ (or $\frac{|\tilde{\lambda}|^2}{(4\pi)^2}$) and we omit them here.

The shift in the coupling induces a shift in R_b according to

$$\frac{\delta R_b}{R_b} \approx 1.5 \frac{\delta g_{d_L}}{g_{d_L}}. \quad (46)$$

The experimental 1σ bound is $\delta R_b/R_b \lesssim 0.003$ [42] which is satisfied in our model for $M \gtrsim 70$ GeV. Thus, our model parameters in both cases II and VI are unconstrained by R_b in the relevant parameter space.

6 Additional collider constraints

6.1 Single top production

D0 have performed a model-independent measurement of the tbq production cross section, where q is a light quark [48]:

$$\sigma(p\bar{p} \rightarrow tbq + X) = 2.90 \pm 0.59 \text{ pb}, \quad (47)$$

in good agreement with the SM t -channel tbq result of 2.26 ± 0.12 pb [49].

In the cases II and VI, single tops can be produced by the process $qg \rightarrow t\phi$, where $q = u, d$. We find the matrix element for such a process to be given by

$$\overline{|\mathcal{M}|^2}_{gu \rightarrow t\phi^0} = -\frac{|\lambda|^2 g_s^2}{3} \left[\frac{\tilde{s}}{\tilde{u}} + \frac{\tilde{u}}{\tilde{s}} + \frac{2(\tilde{t} + \tilde{s})(\tilde{t} + \tilde{u})}{\tilde{u}\tilde{s}} - \frac{2m_t^2}{\tilde{u}^2}(M^2 - m_t^2) \right], \quad (48)$$

where $M = m_0$. For the process $gd \rightarrow t\phi^-$ the replacement $\lambda \rightarrow \tilde{\lambda}$ should be made, and $M = m_+$. The parton level Mandelstam variables obey $\tilde{u} + \tilde{t} + \tilde{s} = M^2 - m_t^2$.

Note, however, that in case II, ϕ^0 that is produced together with the top quark will decay into an up-sector quark and an up-sector antiquark. In case VI, ϕ^- that is produced with the top quark, will decay into the down quark and an up-sector antiquark. In either case, the scalar doublet will not decay into a bottom (anti)quark.

In principle, such a process might still be constrained by the tbq measurement, since the data used in the analysis included a singly b -tagged sample as well. We find that the cross section for the production of $t\phi$ is sizable, of order 3 pb in the allowed parameter space for $A^{t\bar{t}}$. Single top production can then become competitive with the other top-related constraints ($t\bar{t}$ cross section and $A_i^{t\bar{t}}$).

Additionally, the CMS collaboration has recently reported a similar measurement at the LHC [50]:

$$\sigma_t = 84 \pm 30 \text{ pb}, \quad (49)$$

consistent with the SM t -channel result of 64.3 ± 2.2 pb [51]. The cross section of $t\phi$ at the LHC in the allowed parameter space for $A^{t\bar{t}}$ is again sizable, of order 140 – 170 pb.

Given the complexity of the analyses in [48] and [50], and the different kinematics of single top production in our model compared to the SM, a direct comparison of the single top production cross section in our model to Eqs. (47) and (49) is potentially misleading. We find that a dedicated study is required in order to establish the applicability of the single top measurements at the Tevatron and LHC to our model.

6.2 Top decay

If the extra scalar masses are light enough, new decay channels open for the top:

$$\begin{aligned} \Gamma(t \rightarrow \phi^0 u_i) &= \frac{m_t}{8\pi} \left(1 - \frac{m_0^2}{m_t^2}\right)^2 (|X_{i3}|^2 + |X_{3i}|^2), \\ \Gamma(t \rightarrow \phi^+ d_i) &= \frac{m_t}{8\pi} \left(1 - \frac{m_+^2}{m_t^2}\right)^2 (|(V^\dagger X)_{i3}|^2 + |\tilde{X}_{3i}|^2). \end{aligned} \quad (50)$$

In cases II and VI we then have

$$\begin{aligned} \left. \frac{\delta\Gamma_t}{\Gamma_t^{\text{SM}}} \right|_{\text{II}} &\approx 5.2 \left(1 - \frac{m_0^2}{m_t^2}\right)^2 |\lambda|^2, \\ \left. \frac{\delta\Gamma_t}{\Gamma_t^{\text{SM}}} \right|_{\text{IV}} &\approx 5.2 \left(1 - \frac{m_+^2}{m_t^2}\right)^2 |\tilde{\lambda}|^2, \end{aligned} \quad (51)$$

using $\Gamma_t^{\text{SM}} \approx 1.3$ GeV. The direct measurement of the top-quark width puts an upper bound of $\Gamma_t < 7.6$ GeV [52]. A model-dependent indirect measurement of the total top width, from the partial decay width $\Gamma(t \rightarrow Wb)$ measured using the t -channel cross section for single top quark production and from the branching fraction $\text{BR}(t \rightarrow Wb)$ gives $\Gamma_t = 1.99_{-0.55}^{+0.69}$ GeV [53]. We find that measurements of the top width do not constrain the parameter space of our model relevant for producing the forward-backward asymmetry.

The above modification of the top width can effect measurements of the single top and $t\bar{t}$ production cross sections which typically assume SM Wb final states.³ A sizable branching fraction of the top into three light quarks, as predicted in our scenario, might be translated into a reduction in the inferred cross section. This reduction effect might become comparable in magnitude to the scalar exchange contributions in some of the parameter space relevant for $A^{t\bar{t}}$ and cancellations may occur. A naive bound on the size of this effect can be obtained by assuming that the non-SM top decays completely evade the experimental analyses. In this limit, we find that the allowed parameter space shifts to larger values of $\lambda \gtrsim 1$ for roughly the same masses $M \sim 100 - 130$ GeV. The $t\phi$ production cross section is further enhanced in this naive estimate, and so clarifying the applicability of the single top measurements to our model becomes more urgent.

6.3 Same sign tops

Production of same sign tops at the Tevatron due to the couplings of interest to us is negligible. The reason is that the same sign top production is proportional to the product of the couplings of Eq. (10) [case I] and of Eq. (11) [case II]. However, neutral meson-mixing requires that the couplings of Eq. (10) are strongly suppressed. Thus, production of same sign tops [54] does not constrain the parameter space of our models. (The contribution from weak doublet scalar exchange to same sign tops was considered in Ref. [13]. The large effects that they derive arise in the region that is excluded by flavor constraints.)

6.4 Dijet constraints

The weak doublet contributes to dijet production via both t - and s -channel exchange of ϕ^0 . There are no dijet constraints on the model from the Tevatron, since for $M \sim 100 - 130$ GeV the Tevatron has large SM dijet backgrounds [55]. In principle, bounds could arise from measurements by the UA2 collaboration at the CERN SPS collider [56]. However, the t -channel exchange would not have been picked up by the UA2 search, and the s -channel exchange is strongly suppressed by CKM factors, $\sim V_{ub}^2$ (or V_{cb}^2 , paying the price of one c quark pdf). We conclude that dijet constraints from $p\bar{p}$ colliders play no role here.

As concerns the LHC, contributions to dijet production from the s - and t -channels of $gu \rightarrow q\Phi \rightarrow$ dijets resemble non-dominant QCD backgrounds and are not constrained by the dijet angular distribution studies presented by CMS [57] and ATLAS [58].

7 Summary

We investigated whether the large value reported by CDF for the forward backward asymmetry in $t\bar{t}$ production at large invariant mass $M_{t\bar{t}}$ can be accounted for by tree level scalar exchange. We considered top-related measurements, flavor constraints, and electroweak precision measurements. We reached the following conclusions:

- Out of the eight possible scalar representations that are relevant to $A^{t\bar{t}}$, only the color-singlet weak-doublet $\Phi(1, 2)_{-1/2}$ can enhance $A_h^{t\bar{t}}$ and remain consistent with the total and differential $t\bar{t}$ cross section. Roughly speaking, the relevant Yukawa coupling should be $\mathcal{O}(1)$, and the mass of the scalar should be below ~ 130 GeV.

³We thank Pedro Schwaller for a comment on this point.

- Two types of couplings of Φ can contribute to $u\bar{u} \rightarrow t\bar{t}$: $X_{13}q_{L1}^\dagger\Phi t_R$ and $X_{31}q_{L3}^\dagger\Phi u_R$. There is no tension with the differential or total $t\bar{t}$ production cross section. Both couplings are constrained by flavor physics:
 1. The X_{13} coupling is strongly constrained by $K^0 - \bar{K}^0$ and/or $D^0 - \bar{D}^0$ mixing, and so cannot generate a large $A^{t\bar{t}}$.
 2. The X_{31} coupling is not strongly constrained by neutral meson mixing, or by R_b . If ϕ^- couples to the three left-handed down generations with CKM-like suppression $\mathcal{O}(V_{tq})$, then it contributes to the branching ratio of $\bar{B}^0 \rightarrow \pi^+ K^-$ more than two orders of magnitude above the experimental bounds. If, on the other hand, the X_{31} coupling is carefully aligned so that ϕ^- couples only to b_L (but not to s_L and d_L), then it can be large enough to explain $A^{t\bar{t}}$.
- Φ could also affect $A^{t\bar{t}}$ by mediating $d\bar{d} \rightarrow t\bar{t}$ with coupling $\tilde{X}_{31}q_{L3}^\dagger\Phi d_R$. The coupling would need to be bigger than the X_{31} coupling to overcome the small $d\bar{d}$ luminosity at the Tevatron. This is in tension with the $t\bar{t}$ production cross section. Again, flavor constraints are very restrictive:
 1. Similarly to the case of X_{31} , there is no strong constraint from either neutral meson mixing or R_b . If ϕ^0 couples to the three left-handed down generations with CKM-like suppression $\mathcal{O}(V_{tq})$, then it contributes to the branching ratio of $B^- \rightarrow \pi^- \bar{K}^0$ more than two orders of magnitude above the experimental bound. If, on the other hand, the \tilde{X}_{31} coupling is carefully aligned so that ϕ^0 couples only to b_L (but not to s_L and d_L), then it can be large enough to explain $A^{t\bar{t}}$.
 2. The X_{31} and \tilde{X}_{31} couplings cannot be simultaneously order one, because then the upper bound on the branching ratio of $B^+ \rightarrow D^{*+}\pi^0$ is violated by more than two orders of magnitude.

Thus, the coupling \tilde{X} cannot play a significant role in explaining $A^{t\bar{t}}$.

- The flavor constraints that we derive might be circumvented if the contributions to flavor changing processes cancel against contributions from additional scalar doublets. For this to happen, special relations between the couplings of the various scalars must apply. Such relations might appear in models of minimal flavor violation. An example can be found in Ref. [16]. (To fully satisfy the flavor constraints, degeneracy constraints on the scalar spectrum of this model should hold.)
- The new physics contribution to single top production at the Tevatron and LHC is comparable to or larger than the electroweak SM single top production; However the event topology is different. The sensitivity of existing experimental searches, designed to extract SM-like event topologies, to single top production in the weak-doublet model is hard to assess, and a dedicated study is required.
- No sizable distortion of the differential or inclusive $t\bar{t}$ production cross section is expected at the LHC.

We conclude that the interplay between collider physics and flavor physics singles out a weak-scale color-singlet weak-doublet scalar, with a very non-generic flavor structure of Yukawa couplings, as the only viable candidate among the scalars to account for a large forward backward asymmetry in $t\bar{t}$ production.

A Calculating the $t\bar{t}$ production cross section

The details of the calculation of the $t\bar{t}$ production cross section are collected here. We use the following (over-complete) Lorentz basis for the relevant four-fermi flavor conserving operators:

$$\mathcal{O}_{V_q V_t} = \bar{q}\gamma^\mu q \bar{t}\gamma_\mu t, \quad \mathcal{O}_{A_q A_t} = \bar{q}\gamma^\mu \gamma^5 q \bar{t}\gamma_\mu \gamma^5 t, \quad \mathcal{O}_{A_q V_t} = \bar{q}\gamma^\mu \gamma^5 q \bar{t}\gamma_\mu t, \quad \mathcal{O}_{V_q A_t} = \bar{q}\gamma^\mu q \bar{t}\gamma_\mu \gamma^5 t, \quad (52a)$$

$$\mathcal{O}_{S_q S_t} = \bar{q}q \bar{t}t, \quad \mathcal{O}_{P_q P_t} = \bar{q}\gamma^5 q \bar{t}\gamma^5 t, \quad \mathcal{O}_{P_q S_t} = i \bar{q}\gamma^5 q \bar{t}t, \quad \mathcal{O}_{S_q P_t} = i \bar{q}q \bar{t}\gamma^5 t, \quad (52b)$$

$$\mathcal{O}_{T_q T_t} = \bar{q}\sigma^{\mu\nu} q \bar{t}\sigma^{\mu\nu} t, \quad \mathcal{O}_{T'_q T'_t} = \bar{q}\sigma^{\mu\nu} \gamma^5 q \bar{t}\sigma^{\mu\nu} \gamma^5 t, \quad \mathcal{O}_{T'_q T_t} = i \bar{q}\sigma^{\mu\nu} \gamma^5 q \bar{t}\sigma^{\mu\nu} t, \quad \mathcal{O}_{T_q T'_t} = i \bar{q}\sigma^{\mu\nu} q \bar{t}\sigma^{\mu\nu} \gamma^5 t, \quad (52c)$$

with $\sigma^{\mu\nu} = \frac{i}{2} [\gamma^\mu, \gamma^\nu]$. We work with the signature of Peskin and Schroeder [59].

For color contraction, we use the singlet and octet projections as our basis and define:

$$\mathcal{O}_{XY}^8 = (T^a)_i^j (T^a)_k^l (\bar{q}^i \Gamma_{Xq} q_j) (\bar{t}^k \Gamma_{Yt} t_l), \quad \mathcal{O}_{XY}^1 = \frac{\sqrt{2}}{3} \delta_i^j \delta_k^l (\bar{q}^i \Gamma_{Xq} q_j) (\bar{t}^k \Gamma_{Yt} t_l). \quad (53)$$

Then, the coefficients of the four-quark operators are given by

$$\mathcal{L}_{\text{eff}, XY} = \frac{1}{M^2} (c_{XY}^8 \mathcal{O}_{XY}^8 + c_{XY}^1 \mathcal{O}_{XY}^1). \quad (54)$$

The basis Eq. (52) does not respect $SU(2)_L$. It is useful because interference with the SM is proportional to $c_{V_q V_t}^8$ and $c_{A_q A_t}^8$.

The following Fierz identities are useful to our analysis:

$$(\psi_{2R} \psi_{4R}) (\psi_{1R}^\dagger \psi_{3R}^\dagger) = \frac{1}{2} (\bar{\Psi}_1 \gamma^\mu P_R \Psi_2) (\bar{\Psi}_3 \gamma_\mu P_R \Psi_4), \quad (55a)$$

$$(\psi_{1L}^\dagger \psi_{4R}) (\psi_{3R}^\dagger \psi_{2L}) = -\frac{1}{2} (\bar{\Psi}_1 \gamma^\mu P_L \Psi_2) (\bar{\Psi}_3 \gamma_\mu P_R \Psi_4). \quad (55b)$$

Similar identities hold with $L \leftrightarrow R$.

We next write the relevant Lagrangian terms for each of the eight scalar representations listed in Eq. (2), and then the effective four-fermi operators contributing to $t\bar{t}$ production generated by integrating out the scalar field. The effective Lagrangian defined in this way is useful also in the case of light new scalars. The key point here is that only a single diagram contributes to $t\bar{t}$ production cross section for a given representation. Thus it is straightforward to extend the effective Lagrangian to include the momentum dependence of the scalar propagator: One has to simply replace $M^2 \rightarrow M^2 - q^2 - iM\Gamma$. The anti-sextet and the triplet contribute to $u\bar{u} \rightarrow t\bar{t}$ (or $d\bar{d} \rightarrow t\bar{t}$) via u -channel exchange: $q^2 = u = m_t^2 - \frac{s}{2} (1 + \beta_t \cos \theta) = m_t^2 + \tilde{u}$. The octet and the singlet contribute to $u\bar{u} \rightarrow t\bar{t}$ (or $d\bar{d} \rightarrow t\bar{t}$) via t -channel exchange: $q^2 = t = m_t^2 - \frac{s}{2} (1 - \beta_t \cos \theta) = m_t^2 + \tilde{t}$. We neglect $SU(2)$ -breaking mass splittings between the members of the scalar multiplet.

- **Color-sextet weak-singlet** $\Phi \sim (\bar{6}, 1)_{-4/3}$

$$\mathcal{L}^{(\bar{6}, 1)_{-4/3}} = -M^2 \Phi^{ij} \Phi_{ij}^\dagger + \left[2\sqrt{2} \lambda \Phi^{ij} u_{Ri} t_{Rj} + \text{h.c.} \right], \quad (56)$$

$$\begin{aligned} \mathcal{L}_{\text{eff}}^{\bar{6}} &= \frac{|\lambda|^2}{M^2} [\mathcal{O}_{V_u V_t}^8 + \mathcal{O}_{A_u A_t}^8 + \mathcal{O}_{A_u V_t}^8 + \mathcal{O}_{V_u A_t}^8] \\ &+ (\mathcal{O}^8 \rightarrow \sqrt{2} \mathcal{O}^1). \end{aligned} \quad (57)$$

- **Color-sextet weak-singlet** $\Phi \sim (\bar{6}, 1)_{-1/3}$

$$\mathcal{L}^{(\bar{6},1)_{-1/3}} = -M^2 \Phi^{ij} \Phi_{ij}^\dagger + 2\sqrt{2} [\lambda_1 \Phi^{ij} d_{Ri} t_{Rj} + \lambda_2 \Phi^{ij} (q_{Li} Q_{Lj}) + \text{h.c.}], \quad (58)$$

$$\begin{aligned} \mathcal{L}_{\text{eff}}^{\bar{6}} &= \frac{|\lambda_1|^2}{M^2} [\mathcal{O}_{V_d V_t}^8 + \mathcal{O}_{A_d A_t}^8 + \mathcal{O}_{A_d V_t}^8 + \mathcal{O}_{V_d A_t}^8] \\ &+ \frac{|\lambda_2|^2}{M^2} [\mathcal{O}_{V_d V_t}^8 + \mathcal{O}_{A_d A_t}^8 - \mathcal{O}_{A_d V_t}^8 - \mathcal{O}_{V_d A_t}^8] \\ &- \frac{3\Re[\lambda_1 \lambda_2^*]}{M^2} [\mathcal{O}_{S_d S_t}^8 + \mathcal{O}_{P_d P_t}^8] - \frac{3\Im[\lambda_1 \lambda_2^*]}{M^2} [\mathcal{O}_{S_d P_t}^8 + \mathcal{O}_{P_d S_t}^8] \\ &- \frac{\Re[\lambda_1 \lambda_2^*]}{4M^2} [\mathcal{O}_{T_d T_t}^8 + \mathcal{O}_{T_d' T_t'}^8] - \frac{\Im[\lambda_1 \lambda_2^*]}{4M^2} [\mathcal{O}_{T_d T_t'}^8 + \mathcal{O}_{T_d' T_t'}^8] \\ &+ (\mathcal{O}^8 \rightarrow \sqrt{2} \mathcal{O}^1). \end{aligned} \quad (59)$$

The possibility of $\lambda_1 \lambda_2 = \mathcal{O}(1)$ makes the numerical analysis of this model nontrivial. However, note that the coupling λ_2 is subject to strong constraints from flavor physics, including meson mixing and b decays. We simplify the analysis by imposing the conservative constraint $|\lambda_2|^4 (M/\text{TeV})^{-2} < 10^{-2}$.

- **Color-sextet weak-triplet** $\Phi \sim (\bar{6}, 3)_{-1/3}$

$$\mathcal{L}^{(\bar{6},3)_{-1/3}} = -M^2 \Phi^{ij} \Phi_{ij}^\dagger + [2\sqrt{2} \lambda \Phi^{ij} \cdot (q_{Li} Q_{Lj}) + \text{h.c.}], \quad (60)$$

$$\begin{aligned} \mathcal{L}_{\text{eff}}^{\bar{6}} &= \frac{|\lambda|^2}{M^2} [\mathcal{O}_{V_u V_t}^8 + \mathcal{O}_{A_u A_t}^8 - \mathcal{O}_{A_u V_t}^8 - \mathcal{O}_{V_u A_t}^8] + \frac{1}{2} \times (u \leftrightarrow d) \\ &+ (\mathcal{O}^8 \rightarrow \sqrt{2} \mathcal{O}^1). \end{aligned} \quad (61)$$

- **Color-triplet weak-singlet** $\Phi \sim (3, 1)_{-4/3}$

$$\mathcal{L}^{(3,1)_{-4/3}} = -M^2 \Phi_i \Phi^{\dagger i} + [2\lambda \epsilon^{ijk} \Phi_i u_{Rj} t_{Rk} + \text{h.c.}], \quad (62)$$

$$\begin{aligned} \mathcal{L}_{\text{eff}}^3 &= -\frac{|\lambda|^2}{M^2} [\mathcal{O}_{V_u V_t}^8 + \mathcal{O}_{A_u A_t}^8 + \mathcal{O}_{A_u V_t}^8 + \mathcal{O}_{V_u A_t}^8] \\ &+ (\mathcal{O}^8 \rightarrow -\frac{1}{\sqrt{2}} \mathcal{O}^1). \end{aligned} \quad (63)$$

- **Color-triplet weak-singlet** $\Phi \sim (3, 1)_{-1/3}$

$$\mathcal{L}^{(3,1)_{-1/3}} = -M^2 \Phi_i \Phi^{\dagger i} + [2\lambda_1 \epsilon^{ijk} \Phi_i d_{Rj} t_{Rk} + 2\lambda_2 \epsilon^{ijk} \Phi_i (q_{Lj} Q_{Lk}) + \text{h.c.}], \quad (64)$$

$$\begin{aligned} \mathcal{L}_{\text{eff}}^3 &= -\frac{|\lambda_1|^2}{M^2} [\mathcal{O}_{V_d V_t}^8 + \mathcal{O}_{A_d A_t}^8 + \mathcal{O}_{A_d V_t}^8 + \mathcal{O}_{V_d A_t}^8] \\ &- \frac{|\lambda_2|^2}{M^2} [\mathcal{O}_{V_d V_t}^8 + \mathcal{O}_{A_d A_t}^8 - \mathcal{O}_{A_d V_t}^8 - \mathcal{O}_{V_d A_t}^8] \\ &+ \frac{3\Re[\lambda_1 \lambda_2^*]}{M^2} [\mathcal{O}_{S_d S_t}^8 + \mathcal{O}_{P_d P_t}^8] + \frac{3\Im[\lambda_1 \lambda_2^*]}{M^2} [\mathcal{O}_{S_d P_t}^8 + \mathcal{O}_{P_d S_t}^8] \\ &+ \frac{\Re[\lambda_1 \lambda_2^*]}{4M^2} [\mathcal{O}_{T_d T_t}^8 + \mathcal{O}_{T_d' T_t'}^8] + \frac{\Im[\lambda_1 \lambda_2^*]}{4M^2} [\mathcal{O}_{T_d T_t'}^8 + \mathcal{O}_{T_d' T_t'}^8] \\ &+ (\mathcal{O}^8 \rightarrow -\frac{1}{\sqrt{2}} \mathcal{O}^1). \end{aligned} \quad (65)$$

As in the case of the $q_L Q_L$ coupling of the $(\bar{6}, 1)_{-\frac{1}{3}}$ representation, we simplify the analysis by imposing the conservative flavor physics constraint $|\lambda_2|^4 (M/\text{TeV})^{-2} < 10^{-2}$.

- **Color-triplet weak-triplet** $\Phi \sim (3, 3)_{-1/3}$

$$\mathcal{L}^{(3,3)_{-1/3}} = -M^2 \Phi_i \Phi^{\dagger i} + [2\lambda \epsilon^{ijk} \Phi_i \cdot (q_{Lj} Q_{Lk}) + \text{h.c.}], \quad (66)$$

$$\begin{aligned} \mathcal{L}_{\text{eff}}^3 &= -\frac{|\lambda|^2}{M^2} [\mathcal{O}_{V_u V_t}^8 + \mathcal{O}_{A_u A_t}^8 - \mathcal{O}_{A_u V_t}^8 - \mathcal{O}_{V_u A_t}^8] + \frac{1}{2} \times (u \leftrightarrow d) \\ &+ \left(\mathcal{O}^8 \rightarrow -\frac{1}{\sqrt{2}} \mathcal{O}^1 \right). \end{aligned} \quad (67)$$

- **Color-singlet weak-doublet** $\Phi \sim (1, 2)_{-1/2}$

$$\mathcal{L}^{(1,2)_{-1/2}} = -M^2 \Phi^\dagger \Phi + 2 \left[\lambda_1 q_L^{\dagger i} \Phi t_{Ri} + \lambda_2 Q_L^{\dagger i} \Phi u_{Ri} + \lambda_3 Q_L^{\dagger i} \tilde{\Phi} d_{Ri} + \text{h.c.} \right], \quad (68)$$

$$\begin{aligned} \mathcal{L}_{\text{eff}}^1 &= -\frac{|\lambda_1|^2}{M^2} [\mathcal{O}_{V_u V_t}^8 - \mathcal{O}_{A_u A_t}^8 - \mathcal{O}_{A_u V_t}^8 + \mathcal{O}_{V_u A_t}^8] + (u \leftrightarrow d) \\ &- \frac{|\lambda_2|^2}{M^2} [\mathcal{O}_{V_u V_t}^8 - \mathcal{O}_{A_u A_t}^8 + \mathcal{O}_{A_u V_t}^8 - \mathcal{O}_{V_u A_t}^8] + (t \leftrightarrow b) \\ &- \frac{|\lambda_3|^2}{M^2} [\mathcal{O}_{V_d V_t}^8 - \mathcal{O}_{A_d A_t}^8 + \mathcal{O}_{A_d V_t}^8 - \mathcal{O}_{V_d A_t}^8] + (t \leftrightarrow b) \\ &+ \left(\mathcal{O}^8 \rightarrow \frac{1}{2\sqrt{2}} \mathcal{O}^1 \right). \end{aligned} \quad (69)$$

Here, some comments are in order. As found in Section 4, flavor constraints imply that $\lambda_1 \ll 1$ and $\lambda_2 \lambda_3 \ll 1$, while λ_2 or $\lambda_3 = \mathcal{O}(1)$ in order to produce the forward-backward asymmetry. We thus omit in (69) terms proportional to $\lambda_1 \lambda_2^*$ generating same sign tops and single top production at the LHC. When the spectrum of Φ breaks $SU(2)_L$, additional terms of $\mathcal{O}(\lambda_1 \lambda_2)$ adding to $t\bar{t}$ production also appear but are again suppressed and hence omitted. We similarly neglect terms of $\mathcal{O}(\lambda_2 \lambda_3)$ in the above. If one goes beyond the scope of the current work to incorporate flavor symmetries, a sizable λ_1 may become allowed, and the additional $SU(2)_L$ breaking terms should be considered as well.

- **Color-octet weak-doublet** $\Phi \sim (8, 2)_{-1/2}$

$$\mathcal{L}^{(8,2)_{-1/2}} = -M^2 \Phi_a^\dagger \Phi_a + 2\sqrt{6} (T^a)_i^j \left[\lambda_1 q_L^{\dagger i} \Phi_a t_{Rj} + \lambda_2 Q_L^{\dagger i} \Phi_a u_{Rj} + \lambda_3 Q_L^{\dagger i} \tilde{\Phi}_a d_{Rj} + \text{h.c.} \right], \quad (70)$$

$$\begin{aligned} \mathcal{L}_{\text{eff}}^8 &= \frac{|\lambda_1|^2}{M^2} [\mathcal{O}_{V_u V_t}^8 - \mathcal{O}_{A_u A_t}^8 - \mathcal{O}_{A_u V_t}^8 + \mathcal{O}_{V_u A_t}^8] + (u \leftrightarrow d) \\ &+ \frac{|\lambda_2|^2}{M^2} [\mathcal{O}_{V_u V_t}^8 - \mathcal{O}_{A_u A_t}^8 + \mathcal{O}_{A_u V_t}^8 - \mathcal{O}_{V_u A_t}^8] + (t \leftrightarrow b) \\ &+ \frac{|\lambda_3|^2}{M^2} [\mathcal{O}_{V_d V_t}^8 - \mathcal{O}_{A_d A_t}^8 + \mathcal{O}_{A_d V_t}^8 - \mathcal{O}_{V_d A_t}^8] + (t \leftrightarrow b) \\ &+ \left(\mathcal{O}^8 \rightarrow -2\sqrt{2} \mathcal{O}^1 \right). \end{aligned} \quad (71)$$

Similarly to the case of the color singlet isodoublet, $SU(2)_L$ breaking could in principle add terms to $\mathcal{L}^{(8,2)_{-1/2}}$, but flavor constraints imply that these terms are subleading.

We define the symmetric and antisymmetric partonic cross sections as follows:

$$\hat{\sigma}_{\pm} = \int_0^1 dc_{\theta} \frac{d\hat{\sigma}}{dc_{\theta}} \pm \int_{-1}^0 dc_{\theta} \frac{d\hat{\sigma}}{dc_{\theta}}. \quad (72)$$

For heavy NP, the dominant contributions to the cross section arise from interference with the SM:

$$\hat{\sigma}_{+}^{\text{int}} = \frac{c_{VV}^8}{M^2} \frac{2\alpha_s \beta_t}{9} \left(1 - \frac{1}{3}\beta_t^2\right), \quad \hat{\sigma}_{-}^{\text{int}} = \frac{c_{AA}^8}{M^2} \frac{\alpha_s \beta_t^2}{9}. \quad (73)$$

with $\beta_t^2 = 1 - 4m_t^2/\tilde{s}$. We take $m_t = 172.5$ GeV.

Collecting the contributions from all of the operators, the differential partonic $t\bar{t}$ production cross section is:

$$\begin{aligned} \frac{d\hat{\sigma}}{dc_{\theta}} &= \frac{\alpha_s \beta_t \left(M^2 + \frac{\tilde{s}}{2} - m_t^2 + \eta \frac{\tilde{s}\beta_t}{2} c_{\theta}\right)}{9 \left[\left(M^2 + \frac{\tilde{s}}{2} - m_t^2 + \eta \frac{\tilde{s}\beta_t}{2} c_{\theta}\right)^2 + M^2 \Gamma^2\right]} \left[\left(1 - \frac{\beta_t^2}{2}\right) c_{VV}^8 + \beta_t c_{AA}^8 c_{\theta} + \frac{\beta_t^2}{2} c_{VV}^8 c_{\theta}^2 \right] \\ &+ \frac{\tilde{s}\beta_t}{144\pi \left[\left(M^2 + \frac{\tilde{s}}{2} - m_t^2 + \eta \frac{\tilde{s}\beta_t}{2} c_{\theta}\right)^2 + M^2 \Gamma^2\right]} \times \Sigma_{1,8} \\ &\left\{ \beta_t^2 c_V^2 + 2(1 - \beta_t^2)(c_{VV}^2 + c_{AV}^2) + c_{PP}^2 + c_{SP}^2 + \beta_t^2(c_{SS}^2 + c_{PS}^2) + 4(c_T^2 + 2c_{TT}c_{T'T'} + 2c_{TT'}c_{T'T}) (1 - \beta_t^2) \right. \\ &+ 2[2(c_{AV}c_{VA} + c_{VV}c_{AA}) - (c_{SS} + c_{PP})(c_{TT} + c_{T'T'}) - (c_{SP} + c_{PS})(c_{T'T} + c_{TT'})] \beta_t c_{\theta} \\ &\left. + [c_V^2 + 8(c_T^2 + 2c_{TT}c_{T'T'} + 2c_{TT'}c_{T'T})] \beta_t^2 c_{\theta}^2 \right\}, \end{aligned} \quad (74)$$

where

$$\eta = \begin{cases} +1, & u\text{-channel,} \\ -1, & t\text{-channel.} \end{cases} \quad (75)$$

We defined

$$\begin{aligned} c_V^2 &= c_{VV}^2 + c_{AA}^2 + c_{AV}^2 + c_{VA}^2 \\ c_T^2 &= c_{TT}^2 + c_{T'T'}^2 + c_{T'T}^2 + c_{T'T'}^2. \end{aligned} \quad (76)$$

Lastly, in writing

$$\Sigma_{1,8} \{ \dots \},$$

we intend that the term in curly brackets should be summed over the two orthogonal color contractions defined in Eq. (53).

Acknowledgments

We thank Cédric Delaunay, Oram Gedalia, Amnon Harel, Alex Kagan, Gilad Perez, Pedro Schwaller, Sean Tulin, Lidija Zivkovic and Jure Zupan for helpful discussions. YN is the Amos de-Shalit chair of theoretical physics and supported by the Israel Science Foundation (ISF) under grant No. 377/07, by the German-Israeli foundation for scientific research and development (GIF), and by the United States-Israel Binational Science Foundation (BSF), Jerusalem, Israel.

References

- [1] T. Aaltonen *et al.* [CDF Collaboration], Phys. Rev. D **83**, 112003 (2011) [arXiv:1101.0034 [hep-ex]].
- [2] L. G. Almeida, G. F. Sterman and W. Vogelsang, Phys. Rev. D **78**, 014008 (2008) [arXiv:0805.1885 [hep-ph]].
- [3] M. T. Bowen, S. D. Ellis and D. Rainwater, Phys. Rev. D **73**, 014008 (2006) [arXiv:hep-ph/0509267].
- [4] O. Antunano, J. H. Kuhn and G. Rodrigo, Phys. Rev. D **77**, 014003 (2008) [arXiv:0709.1652 [hep-ph]].
- [5] V. M. Abazov *et al.* [D0 Collaboration], Phys. Rev. Lett. **100**, 142002 (2008) [arXiv:0712.0851 [hep-ex]];
- [6] T. Aaltonen *et al.* [CDF Collaboration], Phys. Rev. Lett. **101**, 202001 (2008) [arXiv:0806.2472 [hep-ex]].
- [7] B. Grinstein, A. L. Kagan, M. Trott and J. Zupan, Phys. Rev. Lett. **107**, 012002 (2011) [arXiv:1102.3374 [hep-ph]].
- [8] K. M. Patel and P. Sharma, JHEP **1104**, 085 (2011) [arXiv:1102.4736 [hep-ph]].
- [9] Z. Ligeti, G. M. Tavares and M. Schmaltz, JHEP **1106**, 109 (2011) [arXiv:1103.2757 [hep-ph]].
- [10] J. A. Aguilar-Saavedra and M. Perez-Victoria, JHEP **1105**, 034 (2011) [arXiv:1103.2765 [hep-ph]].
- [11] M. I. Gresham, I. W. Kim and K. M. Zurek, Phys. Rev. D **83**, 114027 (2011) [arXiv:1103.3501 [hep-ph]].
- [12] J. Shu, K. Wang and G. Zhu, arXiv:1104.0083 [hep-ph].
- [13] J. A. Aguilar-Saavedra and M. Perez-Victoria, arXiv:1104.1385 [hep-ph].
- [14] A. E. Nelson, T. Okui and T. S. Roy, arXiv:1104.2030 [hep-ph].
- [15] G. Zhu, arXiv:1104.3227 [hep-ph].
- [16] K. S. Babu, M. Frank and S. K. Rai, arXiv:1104.4782 [hep-ph].
- [17] Y. Cui, Z. Han and M. D. Schwartz, arXiv:1106.3086 [hep-ph].
- [18] J. A. Aguilar-Saavedra, M. Perez-Victoria, [arXiv:1107.0841 [hep-ph]].
- [19] L. Vecchi, arXiv:1107.2933 [hep-ph].
- [20] J. Shu, T. M. P. Tait and K. Wang, Phys. Rev. D **81**, 034012 (2010) [arXiv:0911.3237 [hep-ph]].
- [21] A. Arhrib, R. Benbrik and C. H. Chen, Phys. Rev. D **82**, 034034 (2010) [arXiv:0911.4875 [hep-ph]].
- [22] I. Dorsner, S. Fajfer, J. F. Kamenik and N. Kosnik, Phys. Rev. D **81**, 055009 (2010) [arXiv:0912.0972 [hep-ph]].
- [23] D. W. Jung, P. Ko, J. S. Lee and S. h. Nam, Phys. Lett. B **691**, 238 (2010) [arXiv:0912.1105 [hep-ph]].
- [24] J. Cao, Z. Heng, L. Wu and J. M. Yang, Phys. Rev. D **81**, 014016 (2010) [arXiv:0912.1447 [hep-ph]].
- [25] Q. H. Cao, D. McKeen, J. L. Rosner, G. Shaughnessy and C. E. M. Wagner, Phys. Rev. D **81**, 114004 (2010) [arXiv:1003.3461 [hep-ph]].

- [26] T. Aaltonen *et al.* [CDF Collaboration], Phys. Rev. Lett. **102**, 222003 (2009) [arXiv:0903.2850 [hep-ex]].
- [27] V. Ahrens, A. Ferroglia, M. Neubert, B. D. Pecjak and L. L. Yang, JHEP **1009**, 097 (2010) [arXiv:1003.5827 [hep-ph]].
- [28] CDF Collaboration, CDF note 9913, October 19, 2009; C. Schwanenberger, arXiv:1012.2319 [hep-ex].
- [29] D0 Collaboration, D0 note 6037, May 28, 2010.
- [30] N. Kidonakis, Phys. Rev. D **82**, 114030 (2010) [arXiv:1009.4935 [hep-ph]].
- [31] U. Langenfeld, S. Moch and P. Uwer, Phys. Rev. D **80**, 054009 (2009) [arXiv:0906.5273 [hep-ph]]; M. Cacciari, S. Frixione, M. L. Mangano, P. Nason and G. Ridolfi, JHEP **0809**, 127 (2008) [arXiv:0804.2800 [hep-ph]].
- [32] A. D. Martin, W. J. Stirling, R. S. Thorne and G. Watt, Eur. Phys. J. C **63**, 189 (2009) [arXiv:0901.0002 [hep-ph]].
- [33] H. L. Lai *et al.* [CTEQ Collaboration], Eur. Phys. J. C **12**, 375 (2000) [arXiv:hep-ph/9903282].
- [34] K. Blum *et al.*, Phys. Lett. B, in press [arXiv:1102.3133 [hep-ph]].
- [35] S. Jung, A. Pierce and J. D. Wells, Phys. Rev. D **83**, 114039 (2011) [arXiv:1103.4835 [hep-ph]].
- [36] K. Blum, Y. Grossman, Y. Nir and G. Perez, Phys. Rev. Lett. **102**, 211802 (2009) [arXiv:0903.2118 [hep-ph]].
- [37] B. Grinstein, A. L. Kagan, M. Trott and J. Zupan, work in progress.
- [38] G. Isidori, Y. Nir and G. Perez, Ann. Rev. Nucl. Part. Sci. **60**, 355 (2010) [arXiv:1002.0900 [hep-ph]].
- [39] M. Beneke, G. Buchalla, M. Neubert and C. T. Sachrajda, Nucl. Phys. B **606**, 245 (2001) [arXiv:hep-ph/0104110].
- [40] G. Buchalla, A. J. Buras and M. E. Lautenbacher, Rev. Mod. Phys. **68**, 1125 (1996) [arXiv:hep-ph/9512380].
- [41] M. Beneke, G. Buchalla, M. Neubert and C. T. Sachrajda, Phys. Rev. Lett. **83**, 1914 (1999) [arXiv:hep-ph/9905312].
- [42] K. Nakamura *et al.* (Particle Data Group), J. Phys. G **37**, 075021 (2010).
- [43] A. Das *et al.* [Belle Collaboration], Phys. Rev. D **82**, 051103 (2010) [arXiv:1007.4619 [hep-ex]].
- [44] M. Iwabuchi *et al.* [Belle Collaboration], Phys. Rev. Lett. **101**, 041601 (2008) [arXiv:0804.0831 [hep-ex]].
- [45] F. J. Ronga *et al.* [BELLE Collaboration], Phys. Rev. D **73**, 092003 (2006) [arXiv:hep-ex/0604013].
- [46] G. C. Branco, P. M. Ferreira, L. Lavoura, M. N. Rebelo, M. Sher, J. P. Silva, [arXiv:1106.0034 [hep-ph]].
- [47] Q. H. Cao, M. Carena, S. Gori, A. Menon, P. Schwaller, C. E. M. Wagner, L. T. Wang, [arXiv:1104.4776 [hep-ph]].
- [48] V. M. Abazov *et al.* [D0 Collaboration], [arXiv:1105.2788 [hep-ex]].

- [49] N. Kidonakis, Phys. Rev. **D74**, 114012 (2006) [hep-ph/0609287].
- [50] S. Chatrchyan *et al.* [CMS Collaboration], arXiv:1106.3052 [hep-ex].
- [51] N. Kidonakis, Phys. Rev. D **83**, 091503 (2011) [arXiv:1103.2792 [hep-ph]].
- [52] T. Aaltonen *et al.* [CDF Collaboration], Phys. Rev. Lett. **105**, 232003 (2010) [arXiv:1008.3891 [hep-ex]].
- [53] V. M. Abazov *et al.* [D0 Collaboration], Phys. Rev. Lett. **106**, 022001 (2011). [arXiv:1009.5686 [hep-ex]].
- [54] T. Aaltonen *et al.* [CDF Collaboration], CDF note 10466.
- [55] T. Aaltonen *et al.* [CDF Collaboration], Phys. Rev. **D79**, 112002 (2009) [arXiv:0812.4036 [hep-ex]].
- [56] J. Alitti *et al.* [UA2 Collaboration], Nucl. Phys. B **400**, 3 (1993).
- [57] V. Khachatryan *et al.* [CMS Collaboration], Phys. Rev. Lett. **106**, 201804 (2011). [arXiv:1102.2020 [hep-ex]].
- [58] G. Aad *et al.* [ATLAS Collaboration], New J. Phys. **13**, 053044 (2011). [arXiv:1103.3864 [hep-ex]].
- [59] M. E. Peskin and D. V. Schroeder, *Reading, USA: Addison-Wesley (1995) 842 p.*